



Recycling potential of MWCNTs/HDPE nanocomposite filament: 3D printing and mechanical characterization

Sumodh Kumar¹ · M. R. Ramesh¹ · Mrityunjay Doddamani²

Received: 8 September 2022 / Accepted: 22 January 2023 / Published online: 30 January 2023
© Springer Nature Japan KK, part of Springer Nature 2023

Abstract

Fused filament fabrication (FFF) based additive manufacturing (AM) process is a widely used and emerging manufacturing process for polymer-based products. The recycled filaments are realized through wastage generated while extruding the constant diameter feedstock filament, which is otherwise dumped in landfills or incinerated, releasing hazardous and toxic gases that influence the ecological environment. The wastage of these filaments can be eliminated by recycling and reusing them, addressing materials circular economy effectively, presented in this paper. The functionalized MWCNT reinforced HDPE (high-density polyethylene) nanocomposite (NC) is realized through a brabender, which is further used for filament extrusion. The waste/unrecycled (W/UR) and the recycled filaments are checked for quality. The density of the recycled filaments increases compared to the W/UR filament in each extrusion pass. The crystallinity and tensile properties of the recycled filaments increase compared to the W/UR filament with each additional extrusion cycle. Further, these filaments are used for 3D printing, and investigated for density, XRD and tensile tests. It is observed that the density, crystallinity and tensile properties of the recycled prints increase compared to the W/UR print. The tensile strength and modulus of 1 ×, 2 × and 3 × prints are 63.82, 67.11 and 67.76%, and 45.63, 55.34 and 97.81% respectively, higher than those of the W/UR print. The highest tensile strength and modulus are observed for 3 × print which is 67.76 and 97.81% respectively, higher than those of the W/UR print. 3D prints exhibited enhanced performance as compared to their respective filaments. Finally, the present tensile results are mapped on a property chart, and compared with the available HDPE composites.

Keywords Recycling · Nanocomposite · MWCNT · HDPE · 3D Printing · Tensile

Abbreviations

| | |
|--------------|---|
| ρ_H | : Density of HDPE (kg/m ³) |
| ρ_{exp} | : Experimental density (kg/m ³) |
| ρ_{CNT} | : Density of MWCNT (kg/m ³) |
| ρ_{th} | : Theoretical density (kg/m ³) |
| ρ_C | : Density of composite (kg/m ³) |
| W_H | : Weight % of HDPE |
| W_{CNT} | : Weight % of MWCNT |
| d | : Recycled filament diameter (mm) |
| σ | : Standard deviation (mm) |
| n | : No. of samples |

| | |
|-----|---------------------|
| 3D | : Three dimensional |
| 3DP | : 3D printing |

Introduction

As documented by the United Nations high-level panel on challenges, threats and climate change, environmental degradation (depletion of natural resources like water, soil and air, elimination of ecosystems, pollution and extinction of wildlife, which are harmful to the ecosystem) is one of the ten threats affecting the world today [1, 2]. Environmental degradation is mainly due to indiscriminate CO₂ emission. CO₂, a greenhouse gas, is emitted from burning fossil fuels (natural gas, oils, coal), trees, solid waste and other biological waste [3]. Plastic waste is polymer-based products that are carbon-based materials and emit CO₂ into the atmosphere. CO₂ emission leads to global warming, which further leads to climate change resulting in fluctuation in seasons, low rainfall and temperature rise of the environment, causing

✉ Mrityunjay Doddamani
mrityunjay@iitmandi.ac.in

¹ Mechanical Engineering, National Institute of Technology Karnataka, Surathkal, India

² School of Mechanical and Materials Engineering, Indian Institute of Technology Mandi, Mandi 175075, Himachal Pradesh, India

low agricultural output and drought globally. Moreover, some effects of climate change are health problems, severe storms, and rising sea levels affecting coastal areas, migration, and the decreasing economy [4]. These concerns are a major challenge for the world, and finding the appropriate solution for decarbonization, i.e., minimizing CO₂ emissions in the atmosphere is crucial for human survival. Scientists/researchers have taken several steps to provide solutions to the climate change issue like the development of different new materials for the storage of CO₂ and the recommendation for shifting toward renewable energy sources [5–7]. Moreover, reducing deforestation and making the environment free from plastic waste can also minimize CO₂ emissions in the atmosphere. The current work focuses on recycling carbon-based nanocomposite products and reusing them to make the desired products. This will help eliminate plastic waste from the environment and thereby help reduce CO₂ emissions to achieve the carbon neutral society.

The most widely consumed polymer, high-density polyethylene, provides various properties such as mechanical, chemical, and corrosion resistance, making them useful for industrial applications such as aeronautical, automotive, agricultural and domestic products manufacturing industries [8]. Nonetheless, these thermoplastic wastes are non-degradable, causing environmental pollution and affecting the ecological balance [9]. Environmental pollution has become a global issue nowadays, and plastic waste is the major contributor to it as plastic material releases toxic gases in post-usage/consumption. These toxic gases are hazardous to plants, animals and human beings. In our day-to-day life, polymers' usage is increasing, hence the associated wastage. Therefore, reducing the plastic waste is crucial to saving environmental pollution, which can be accomplished by adopting a circular materials approach of recycling and reuse. Recycling is a manufacturing process in which waste material is processed and made useful for polymer-related applications [10]. There are different recycling processes such as mechanical, primary, quaternary and chemical. Among them, mechanical recycling is the most commonly used process as it involves reheating the polymers [11]. Most plastic waste comes from the packaging and daily used products such as straws, plastic bottles and carry bags, which are made of thermoplastic polymers such as polypropylene, polyethylene, polycarbonate and polyvinyl chloride. Therefore, recycling thermoplastic polymers and their composites and reusing them to make different functional components can reduce plastic waste to a large extent. Thermoplastic polymers have unique characteristics and reheating capabilities, which can be recycled and reused for different applications. There are different thermoplastic polymers such as polypropylene [12], polycarbonate [13], polyvinyl chloride [14], polylactic acid [15], acrylonitrile butadiene styrene [16], polyethylene terephthalate [17] and

HDPE [18, 19], used as the matrix in thermoplastic polymer composites. Glass microballoons (GMBs) [20, 21], fly ash cenospheres [22, 23], glass fibers [24], carbon fibers [25], carbon black [26], montmorillonite nanoclay [27], graphene [28] and carbon nanotubes [15, 29] are the common filler materials used to reinforce these thermoplastic polymers.

The advanced manufacturing process such as FFF-based 3DP is the most widely used for thermoplastics manufacturing due to its design flexibility, integrated components, a wide range of filament availability and lower lead times. FFF 3DP process is a layered material deposition through G-code created using a stereolithography (.STL) file where input materials are used in filament [30]. 3DP finds applications in different sectors such as automobile [31], aerospace [32], marine [33] and medical [34]. Due to the wide application areas of 3DP, there is increasing thrust for developing different newer filaments. In 3DP thermoplastic polymers and their composites, warpage is the major concern that can be eliminated by embedding thermally stable reinforcements in the polymer matrix [35–37]. Carbon nanotubes (CNTs) are thermally stable and can reinforce polymer matrix to eliminate the warpage issues posed by the semi-crystalline HDPE. Moreover, they have outstanding mechanical and thermal properties. Additionally, they have a higher aspect ratio and surface area [29]. Due to all these reasons, CNTs become a suitable filler material, and are hence chosen as filler in the current work.

The common thermoplastics used with CNTs are polycarbonate and polyurethane [38], polyethylene [39], polystyrene [40], etc. HDPE has a good mechanical, chemical, wear resistance, impact strength, physical and moderate rigidity properties, and is widely utilized in industries [41, 42]. It is used in chemical containers, packaging industries, household products, jugs and many other applications [30, 36]. HDPE is commonly reinforced with GMBs [36], fly ash cenospheres [23], nanoclay [27], carbon [43], wood flour [44], graphite fibers [45], etc. The small addition of CNTs can enhance the modulus and strength of the 3D printed polymer composites [41]. The composites developed using the CNTs reinforcements are called nanocomposites as the CNTs are of nanosize. These NCs are used in several engineering fields such as automobiles, military, aerospace and naval [29, 46].

Ashish Kumar Singh et al. [20] studied the recycling potential of fly ash cenospheres/HDPE foam (HDPE40). The foam density was observed to increase until the 2nd extrusion cycle due to cenospheres breakage and consolidation of porosities. The tensile moduli and yield strengths of HDPE and HDPE40 filaments increased with additional extrusion passes. Rupinder Singh et al. [47] studied the thermal and tensile properties of an energy storage device (ESD) made up of recycled ABS reinforced with different fillers (graphite, MnO₂, ZnCl₂, and NH₄Cl) fabricated by

3DP. They observed that the ESD has better tensile properties (modulus, strength), and can work in severe loading conditions. Narinder Singh et al. [48] worked on recycling HDPE and extrusion of filaments by reinforcing SiC/Al₂O₃ particles. They investigated thermal, MFI and tensile properties, and found no significant effect of reinforcement on thermal and rheological (MFI) properties. Felicia Stan et al. [49] presented the recycling of LDPE/MWCNT composites fabricated by injection molded method, and investigated rheology mechanical and electrical properties. They observed that shear viscosities of neat and recycled composites decrease with increasing shear rates and MWCNT loading. Further, the shear-thinning behavior is prominently exhibited at high shearing rates. The tensile strength and the composite modulus increased with MWCNT loading. The electrical conductivity shows an increasing trend up to 5 wt. %. Changqing Fang et al. [50] studied the effect of MWCNT addition on recycled PET/TPU composite properties. The tensile strength and thermal stability of the CNTs/rPET/TPU composites improved with increasing CNT content. Rupinder Singh et al. [51] extruded recycled HDPE and LDPE filaments reinforced with Fe powder. Reinforced composites exhibited better properties compared to pure materials. The breaking strength and hardness increased with filler loading.

The prevailing literature reveals that the recycling potential of functionalized MWCNTs reinforced HDPE is yet to be explored. The present work studies the recycling potential of functionalized MWCNTs/HDPE NCs. The waste filaments post-extrusion is recycled once (1x), twice (2x) and thrice (3x) by pelletizing them after every extrusion pass. Subsequently, the recycled filaments are tested for density, XRD and tensile properties to check their enhancement and recycling potential. Further, these developed and recycled filaments are utilized in 3D printing of the NCs, and are subsequently tested for density, XRD and tensile responses to check the property enhancement post-printing. Finally, the tensile properties of the printed samples are compared with HDPE composites.

Experimental

Materials and nanocomposite development method

HD50MA180 (HDPE) granules are used as a matrix. Functionalized MWCNTs produced by the carbon vapor deposition process used as filler is procured from Adnano Tech., India. The typical properties of the functionalized MWCNTs and HDPE are presented in Ref. [42]. Due to the higher aspect ratio, small diameters and entwined bundled form of single-walled CNTs, their uniform distribution in the matrix is difficult. In contrast, the MWCNT (non-functionalized) exhibits inferior interfacial bonding between matrix and

filler, limiting their reinforcement potential [46]. The homogeneous mixing of HDPE and the functionalized MWCNTs is achieved by the blending process using a 16CME SPL Brabender. The mixing speed and the temperature are set at 10 rpm and 210 °C, respectively [33]. 1% (wt.) of the functionalized MWCNTs powder is weighed, mixed with HDPE mechanically, and fed to the hopper of the brabender to obtain NC pellets. The developed functionalized MWCNTs/HDPE NC is designated as H1, and the NC pellets are shown in Fig. 1.

Filament manufacturing and recycling

The NC pellets obtained from Brabender are used to extrude the filament for a 3D printer. A 25SS/MF/26 single screw extruder is used to extrude the filaments, supplied by Aasabi Machinery Pvt. Ltd., Mumbai, having a 25:1 L/D ratio. The barrel temperatures from the feed-die section are 145–150–155–145 °C. Post-stabilization of the temperatures, the NC pellets/blends are fed to the extruder screw through hopper. The screw (24.8 rpm) and the take-off unit speeds (11.0 rpm) are set up to start the extrusion process, and changed together to obtain the desired diameter of the filament. There is a large amount of filament wastage while selecting/choosing the suitable extrusion parameters setting to obtain the filament's desired diameter. In this work, these waste filaments are recycled to reduce the plastic waste from the environment. The waste filaments are collected, pelletized and pre-heated in an oven at 80 °C for 24 h to avoid moisture content before the extrusion of the recycled filaments. The first-time extruded filament is designated as 1x filament. The 1x filament is pelletized, and fed again to obtain a second-time extruded (2x) filament. The same method is repeated to get the third-time extruded filament, which is further designated as 3x filament. Figure 2 presents



Fig. 1 Representative image of MWCNT/HDPE NC pellets

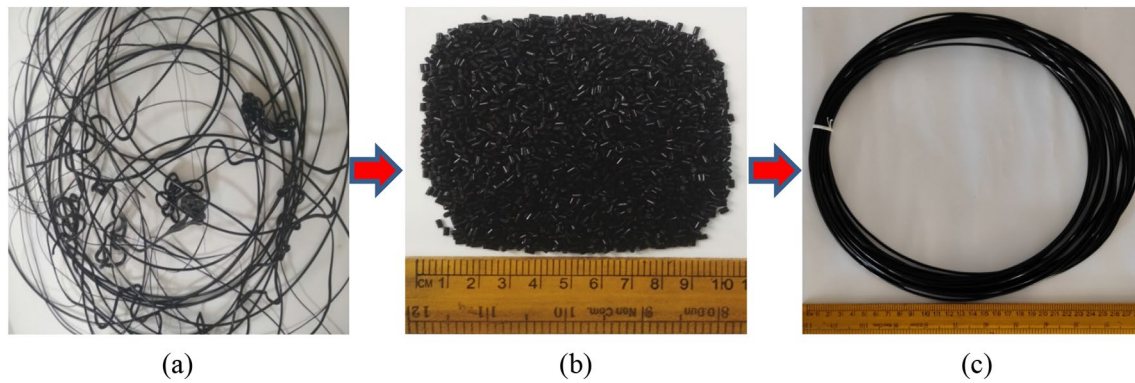


Fig. 2 Representative images of **a** W/UR filament, **b** pellets of W/UR filaments, and **c** H1-3X recycled filament

the waste extrusion filaments, waste filament pellets and 3× recycled filament having a consistent diameter.

Filament regularity check and density measurement

The regularity of the filament cross-section is checked by measuring its diameter and standard deviation. A minimum of five samples from different filament zones of extruded recycled filaments are taken for diameter measurement. The mean/average diameter (\bar{d}) is calculated using [42]

$$\bar{d} = \frac{\sum d_i}{n}, \quad (1)$$

and the deviations (σ) are estimated through [42]

$$\sigma = \sqrt{\frac{\sum (d_i - \bar{d})^2}{n}}. \quad (2)$$

The measurement of the filament density and the prints are carried out using the ASTM D792-20. The theoretical density of the filaments and the prints are calculated with the help of the rule of mixture [42].

$$\rho_c = \frac{1}{\frac{W_H}{\rho_H} + \frac{W_{CNT}}{\rho_{CNT}}}. \quad (3)$$

XRD of the filaments and prints

The crystallinity of the filaments and the printed samples is measured using Malvern PANalytical, the Netherlands (Model-Empyrean 3rd Gen), fitted out with Cu α radiation at 40 mA and 45 kV using a Nickel filter. The samples are scanned at a 2°/min speed from 10 to 80° (2 θ) [52].

Tensile testing of the filaments and prints

The filaments and the prints are tensile tested according to ASTM D638-14 using a Zwick Roell universal testing machine (Z020, load cell: 20 kN, initial load-0.1 MPa) with a 5 mm/min cross-head speed through an extensometer (2-inch gauge length) for strain measurements.

3D Printing of sample

An FFF-based commercial 3D printer supplied by Aha 3D, India (2 nozzles, 0.8 mm diameter), is used to print the samples. The unrecycled and recycled filaments (1×, 2× and 3×) are used to print samples. The NC samples are printed on Kraton™ SEBS FG1901, and left on the build plate to cool to obtain the warpage-free prints [31].

Results and discussion

Filament regularity and quality check

The uniform regularity in the diameter is crucial for the uniform material flow through the printer nozzles resulting in good-quality prints. The mean diameter and the standard deviation of the W/UR and the recycled filament are listed in Table 1. The mean diameter of each filament is 2.73 mm, which shows the extrusion consistency. The standard

Table 1 Density of the filaments and the prints

| Particulars | \bar{d} with σ (mm) | ρ_{th} (kg/m ³) | ρ_{exp} (kg/m ³) | |
|-------------|---------------------------------|----------------------------------|-----------------------------------|-------------|
| | | | Filaments | Prints |
| W/UR | 2.73±0.03 | 898.04 | 901.01±4.20 | 903.18±3.93 |
| 1x | 2.73±0.02 | | 948.42±4.40 | 950.27±2.48 |
| 2x | 2.73±0.01 | | 983.25±7.48 | 986.31±4.35 |
| 3x | 2.73±0.01 | | 985.13±9.61 | 991.43±5.12 |

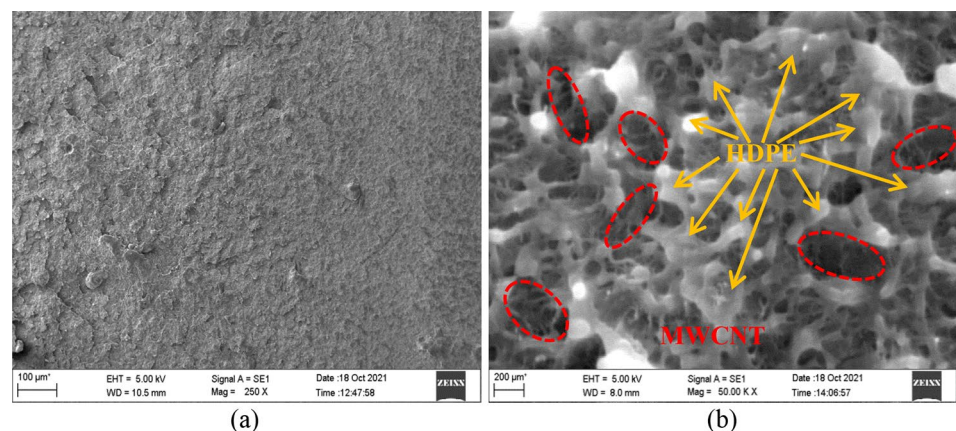
deviation of W/UR filament is higher (0.03 mm) than the recycled filaments (1×, 2× and 3×), which shows that W/UR filament has minor variations in the diameter than the 1×, 2× and 3× filaments. The 2× and 3× (0.01 mm) filament diameter is lower than the 1× filament (0.02 mm), which might be due to the stiffening effect post subsequent thermal cycles. Further, the decrease in standard deviation may be due to the good arrangement of polymer chains and the functionalized MWCNTs in the NCs. There is no change in the standard deviation of 2× and 3× recycled filaments, implying the saturation of polymer chains and the fillers realignment. The higher diameter variations in the W/UR filament compared to the recycled filaments are due to the random alignment of the polymer chains and the functionalized MWCNTs. Further, when the filaments are recycled, the polymer chains and the functionalized MWCNTs undergo thermal processing, where they get aligned. Therefore, the filament cross-section reduces slightly, lowering the standard deviation further. Moreover, the variations in the filament diameter may also be due to matrix porosity. The matrix porosity in the recycled filament reduces the material's tensile strength [36]. The presence of porosity is determined through the density measurement of the sample. The density of the W/UR filament, recycled filament and prints are listed in Table 1. The density of the recycled filaments (1×, 2× and 3×) increases compared to the W/UR filament. It is also observed that the recycled filament density increases with each additional extrusion pass. The maximum density is observed to be for 3× recycled filament. In contrast, the densities of 2× and 3× filaments are approximately the same, showing the delay in the realignment of the polymer chains and the fillers. The same trend is observed for the prints as well. The prints' density is higher than the extruded counterparts, showing the additional alignment of the polymer chains with fibers and the higher time of crystallization in the printing process. The experimental density of the W/UR filament, recycled filament and 3D prints are higher compared to the theoretical density of the H1 nanocomposite,

which shows no air voids/porosity in the sample. This can also be seen in the SEM image of the freeze-fractured H1-3× print. The lower magnification image of H1-3× (Fig. 3a) shows the matrix's air voids/porosity absence. In contrast, the higher magnification image (Fig. 3b) shows the homogeneous dispersion of the functionalized MWCNTs in HDPE.

XRD of the NC filaments and prints

The polymer chains' and fibers' realignment influence the filaments' and prints' crystallinity. The XRD test is performed for the filaments and the prints to check the changes in their crystallinity. The XRD of the developed compositions and associated prints are presented in Fig. 4a and b, respectively, and the corresponding values are presented in Table 2. The peaks intensity of the recycled filaments' increases compared to the W/UR filament. The peak intensity also increases with each extrusion cycle. The peak values (Table 2) show orthorhombic crystal structures at (110) and (200) lattice plane [53]. Similar observations are noted for the prints as well. The highest peak intensity is observed for 3× filament and the print. The sharpness of the peak represents crystallinity. Therefore, the increase in the peak intensity can be correlated to an increase in crystallinity. The degree of crystallinity increases for the filaments and the prints compared to the W/UR filament and the print respectively. It also increases with each extrusion cycle, as clearly evident from Table 2. The increase in the peak intensity and the degree of crystallinity of the filaments and the prints may be due to the realignment of the polymer chains and the fillers while undergoing additional thermal processing. The degree of crystallinity of the prints is higher than the filaments owing to the thermal heating (additional) and the higher time of crystallization in the 3D printing.

Fig. 3 Representative images of 3D printed freeze-fractured H1-3× print at **a** lower and **b** higher magnifications



Tensile test of the NC filaments

The increase in the density and the crystallinity of the recycled filaments compared to the W/UR filament influences the mechanical properties. In the present work, the tensile test is performed on the recycled and W/UR filaments to investigate their tensile properties. Moreover, the tensile test of the filaments is crucial to check their strength and stiffness so that they can be further utilized for 3D printing. The tensile responses of the NC filaments are shown in Fig. 5a and Table 3. The modulus of the recycled filaments (1×, 2× and 3×) increases compared to the W/UR filament. The modulus of 1×, 2× and 3× recycled filaments is 12.74,

20.30 and 23.12%, respectively, higher than the modulus of the W/UR filament. The polymer chains and the functionalized MWCNTs get realigned through the extrusion process, enhancing the adhesion between the filler and matrix, resulting in a higher modulus. The modulus of the recycled filaments also increases with each extrusion pass up to the 3rd, after that, no significant change is observed. The modulus of 2× and 3× filaments is 6.70 and 9.20%, respectively, higher than that of the 1× filament, while the modulus of the 3× filament is 2.34% higher than the modulus of 2× filament, showing the property enhancement saturation. The highest modulus is observed for 3× filament, 23.12% higher than that of the W/UR filament. The increased modulus in

Fig. 4 The XRD pattern of NC **a** filaments and **b** prints

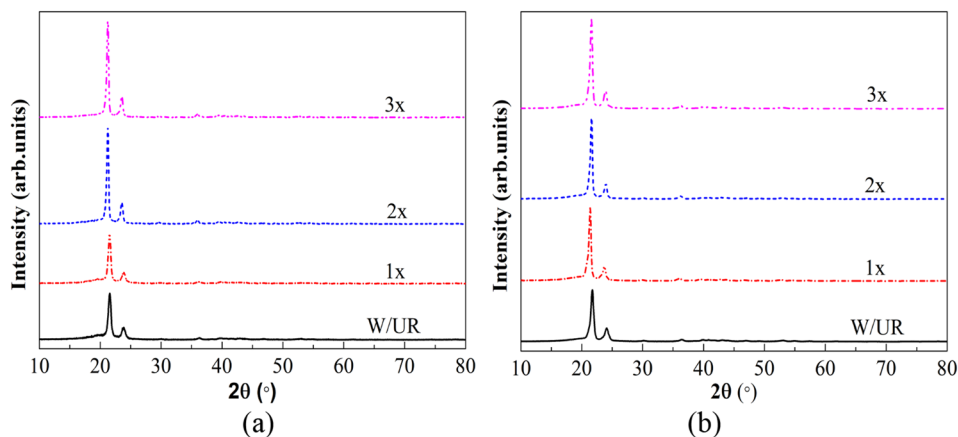


Table 2 The XRD responses of filaments and prints

| Particulars | Filament peak position 2θ (°) | | 3D prints peak position 2θ (°) | | Degree of crystallinity (%) | |
|-------------|-------------------------------|----------|--------------------------------|----------|-----------------------------|-----------|
| | 1st peak | 2nd peak | 1st peak | 2nd peak | Filaments | 3D Prints |
| W/UR | 21.23 | 23.63 | 21.32 | 23.42 | 59.04 | 68.35 |
| 1x | 21.53 | 23.81 | 21.48 | 23.79 | 61.21 | 71.42 |
| 2x | 21.15 | 23.52 | 21.51 | 23.91 | 62.89 | 73.33 |
| 3x | 21.53 | 23.80 | 21.26 | 23.52 | 65.67 | 75.46 |

Fig. 5 Representative **a** tensile stress–strain plot of the NC filaments and **b** SEM image of H1-3× recycled filament

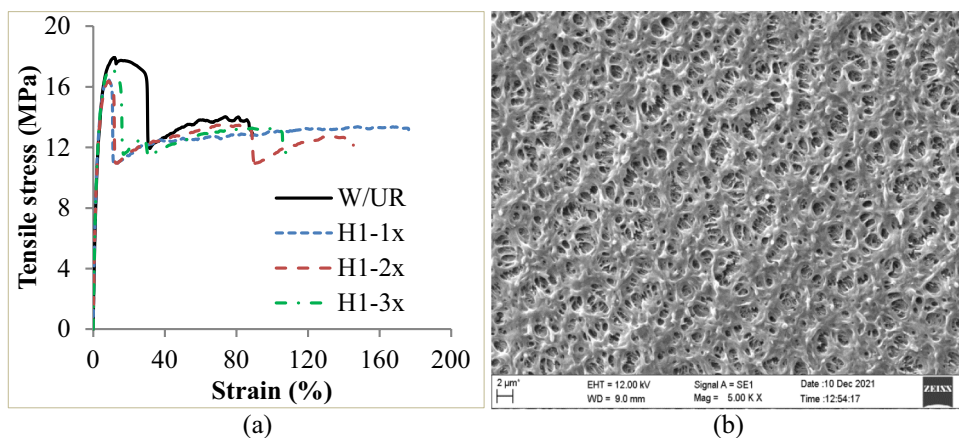


Table 3 Tensile responses of filaments and prints

| Number of cycles | Modulus (MPa) | | Yield strength (MPa) | | UTS (MPa) | | Fracture strength (MPa) | | Fracture strain (%) | |
|------------------|---------------|-------------|----------------------|---------------|--------------|--------------|-------------------------|---------------|---------------------|----------------|
| | Flmt | Print | Flmt | Print | Flmt | Print | Flmt | Print | Flmt | Print |
| W/UR | 675 ±19 | 824 ±26 | 15.9 ±0.6 | 7.86 ±0.4 | 15.9 ±0.6 | 15.2 ±0.5 | 12.87 ±0.6 | 15.0 ±0.9 | 89.22 ±0.6 | 7.64 ±3.31 |
| 1x | 761 ±12 | 1200 ±13 | 16.5 ±0.1 | 12.7 ±0.3 | 16.5 ±0.1 | 24.9 ±0.7 | 12.94 ±0.3 | 24.5 ±0.5 | 176.38 ±3.21 | 12.17 ±2.23 |
| 2x | 812 ±17 | 1280 ±16 | 17.2 ±0.3 | 10.37 ±0.2 | 17.2 ±0.3 | 25.4 ±0.4 | 12.15 ±0.2 | 25.03 ±0.6 | 145.36 ±4.33 | 5.07 ±1.04 |
| 3x | 831 ±15 | 1630 ±23 | 17.4 ±0.2 | 11.71 ±0.3 | 17.4 ±0.2 | 25.5 ±0.3 | 11.35 ±0.5 | 24.87 ±0.2 | 108.42 ±3.94 | 4.70 ±2.06 |

the recycled filaments with each extrusion pass is due to an additional realignment of the polymer chains due to further thermal processing. The yield strength (YS) and the ultimate tensile strength (UTS) of the recycled filaments are the same, and higher than those of the W/UR filament. The YS and UTS of 1×, 2× and 3× recycled filaments are 3.77, 8.17 and 9.43%, respectively, higher than those of the W/UR filament. The recycled filaments' YS and UTS also increase with each extrusion pass. The YS of the 2× and 3× filaments is 4.24 and 5.45%, respectively, higher than that of 1× filament, while the YS of the 3× filament is 1.16% higher than the YS of the 2× filament. The highest YS and UTS are observed for 3× filament (9.43% higher than W/UR filament). YS increases due to the increased crystallinity (as observed in XRD discussions), further increasing the filaments' elasticity (elastic region). The rise in UTS is due to the cross-linking of the polymer chains, which enhances the load transfer capability. The SEM image of the 3× recycled tensile-tested filament is shown in Fig. 5b, showing the cross-linking and the good distribution of the functionalized MWCNTs, and the better bonding between the constituents. The fracture strength of the 1× filament is observed to be the highest. The fracture strain of the recycled filaments (1×, 2× and 3×) is higher than that of the W/UR filament, showing the increased ductility (due to more elongation) of the recycled filaments as compared to the W/UR filament. It can also be observed that the fracture strain of the recycled (1×, 2× and 3×) filaments is reducing with each extrusion pass. This is due to increased brittleness in the recycled filaments while going through each extrusion pass. Overall, the tensile responses show the enhancement in modulus and the strength of the recycled filaments compared to the W/UR filament, which indicates that these filaments can be utilized in 3D printer for components manufacturing for different applications.

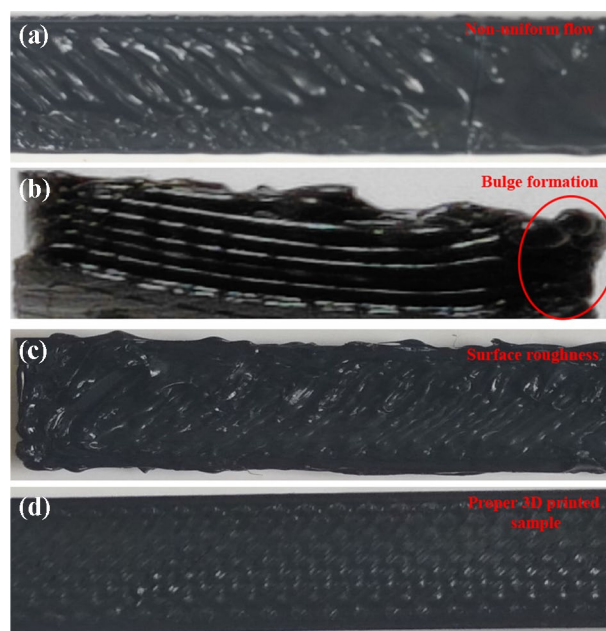
3D printing

Suitable 3D printing parameters are required for good-quality prints. The suitable 3D printing parameters are

Table 4 Suitable 3D printing parameters used in the current work [42, 52]

| Parameters | Values |
|-------------------------|------------------|
| Extrusion multiplier | 0.90–1.0 [0.95] |
| Layer height (mm) | 0.30–0.50 [0.50] |
| Nozzle temperature (°C) | 190–220 [200] |
| Printing speed (mm/s) | 25–35 [30] |

*Values in the square bracket = Suitable 3D printing parameters

**Fig. 6** Challenges encountered in 3DP of recycled filaments

obtained through the pilot studies shown in Table 4 [42, 52], which are set for 3D printing. The samples 3D printed at respective extrusion multipliers of 0.90 and 1.0 showed the non-uniform flow of the material (Fig. 6a). Bulge formation (Fig. 6b) was observed when the samples were printed with layer heights between 0.30 and 0.50 mm. The proper

clearance must be between the two layers to obtain bulge-free samples. Printing temperature is also very crucial for good-quality prints. A higher printing temperature (220 °C) leads to overheating of the samples, and a lower printing temperature (190 °C) leads to improper flow of materials, which further influences the quality of the prints. The samples printed at a higher speed (35 mm/s) increased the surface roughness (Fig. 6c). The samples printed using the suitable parameters showed a good-quality print (Fig. 6d). The W/UR and the recycled filaments (1×, 2× and 3×) are used as feedstock filaments to print samples. The samples printed with W/UR filament are named as waste/unrecycled (W/UR) print, whereas the samples printed with the recycled filaments, 1×, 2× and 3×, are designated as 1×, 2× and 3× prints (recycled prints), respectively. After printing, the samples are tested for density, XRD and tensile properties.

Tensile test of the 3D printed samples

The printability of the W/UR and the recycled filaments is assured through the tensile testing of the filaments, and then used to print tensile samples to check their property enhancement potential. The tensile-tested samples exhibiting the brittle failure (Fig. 7a) and the close-up image of the fractured surface (Fig. 7b) are presented. The tensile responses of the prints are shown in Fig. 8a, and the corresponding values are given in Table 3. The modulus of the recycled printed samples increases compared to the W/UR printed samples. The modulus of 1×, 2× and 3× printed samples is 45.63, 55.34 and 97.81%, respectively, higher than that of the W/UR printed sample. The increase in modulus is due to the higher crystallinity and the constituent elements interfacial bonding enhancement. The modulus of 2× and 3× prints is 6.67 and 35.83%, respectively, higher compared to 1× print, while the modulus of the 3× print is 27.34% higher than the modulus of 2× print. The highest modulus is noted for 3× print, 97.81% higher than that of the W/UR print. The modulus of the printed samples has been observed to be higher with respect to the corresponding modulus of the filaments. The modulus of W/UR, 1×, 2× and 3× prints has been increased by 22.07, 57.69, 57.63 and 96.15%, respectively, compared to the modulus of the respective filaments. This is due to the additional thermal processing of the filaments in the 3D printing process, where the polymer chains are again aligned in addition to the filler functionalization. The recycled printed samples' YS are higher than the W/UR prints. The highest YS is observed for 1× print, and is 61.58% higher than that of the W/UR print. No significant effect in the YS of the printed samples is observed compared to the YS of the respective filaments. The UTS of the recycled prints (1×, 2× and 3× prints) also increases compared to the UTS of the W/UR print. The UTS of 1×, 2× and 3× prints is 63.82, 67.11 and 67.76%, respectively, higher as compared to the W/UR print. The highest UTS is observed for 3× print, 67.76%, which is higher than

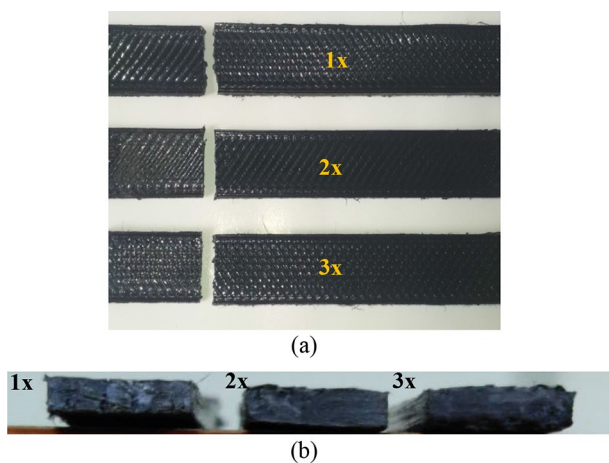
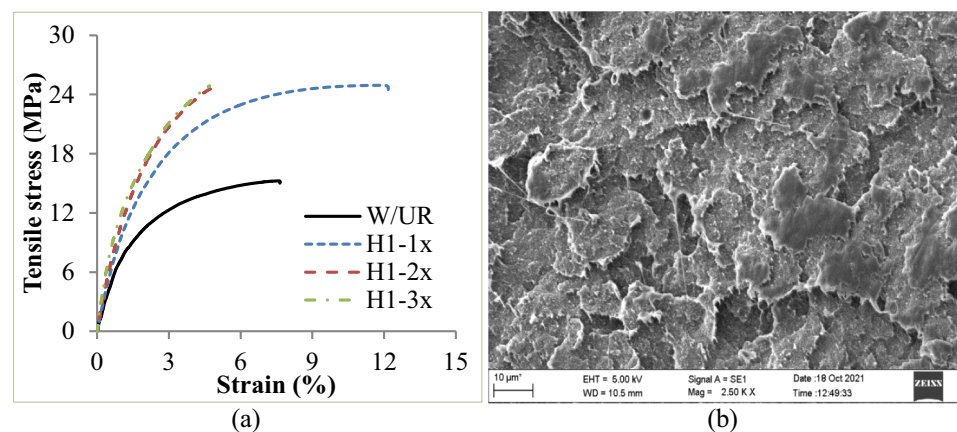


Fig. 7 Tensile-tested samples showing **a** brittle failure and **b** fractured surfaces in brittle mode

Fig. 8 Representative **a** tensile stress–strain graph of the printed samples and **b** SEM image of tensile-tested H1-3× printed sample



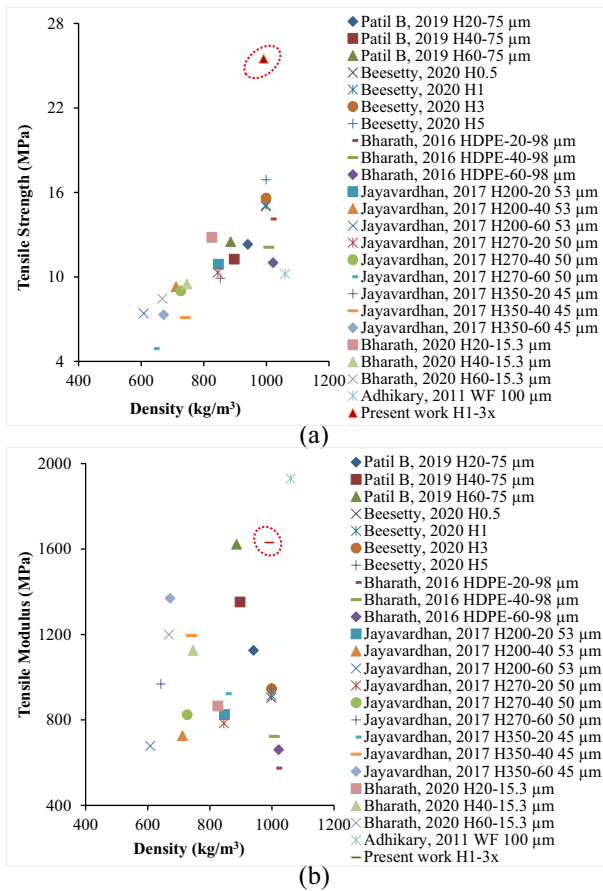


Fig. 9 Comparison of tensile **a** strength and **b** modulus of different HDPE composites with H1-3× composite ([22, 27, 33, 36, 44, 54])

that of the W/UR print. There is no significant change in the UTS of the W/UR filament and the print, whereas the UTS of the recycled prints is observed to be increasing compared to the recycled filaments. The UTS of the 1×, 2× and 3× prints is 50.91, 47.67 and 46.55%, respectively, higher than that of the 1×, 2× and 3× filaments. The increase in UTS may be attributed to the rise in load transfer capability due to additional cross-linking of the polymer chains when it undergoes recycling. The fracture strength of the recycled print is higher in comparison to W/UR print. The fracture strength of the prints is higher than that of the filaments, 16.55, 89.33, 106.01 and 119.12% higher for W/UR, 1×, 2× and 3× prints, respectively, for their respective filaments. The highest fracture strength and strain are observed for 2× and 1× print, 66.87 and 59.29%, respectively, higher than that of the W/UR print. The printed samples undergo the additional extrusion recycling cycle when printed using a 3D printer, where they get more aligned and cross-linked, thereby enhancing the modulus and strength. It is observed that the 3× print is the best sample having the highest modulus, YS, UTS and fracture strength. The SEM image of the tensile-tested 3× printed sample is shown in Fig. 8b.

Property map

The tensile modulus and the strength [22, 27, 33, 36, 44, 54] of the H1-3× printed sample (which is an HDPE-based composite) of the present study have been compared with different HDPE-based composites reinforced with various filler materials and manufactured by different methods against the density of the composites. The tensile modulus and the strength are presented in Fig. 9. The density of the H1-3× printed sample is lower than the nanoclay/HDPE composites [27] and fly ash cenospheres/HDPE composites [33]. The H1-3× print exhibited the highest modulus (Fig. 9a), except for the solid particle-filled HDPE composite. This highest modulus of the H1-3× sample may be due to the good distribution of the functionalized MWCNTs in HDPE and the enhanced interfacial bonding between HDPE and the functionalized MWCNTs. The highest tensile strength (Fig. 9b) is observed for the H1-3× printed sample compared to the other HDPE composites. The highest tensile strength shows that the functionalized MWCNTs are well oriented in HDPE, helping in the effective (highest) load transition from HDPE to the functionalized MWCNTs. The property plot shows that the H1-3× print has more strength than other HDPE composites filled with fillers, like nanoclay, GMB, fly ash cenospheres and wood flour. Moreover, the H1-3× printed sample shows a superior tensile modulus than HDPE composites with GMB, nanoclay and fly ash cenospheres. Thus, the study of the property map reveals that the functionalized MWCNTs/HDPE NCs recyclability potential can be effectively and efficiently exploited through 3D printing method to achieve a wider range of tailored physical and mechanical responses for various applications.

Conclusions

The waste filaments of the functionalized MWCNTs/HDPE NCs are successfully utilized to obtain the recycled filaments, and tested for density, crystallinity and tensile properties. The W/UR and the recycled filaments are used for 3D printing of the samples. The printed samples are subjected to density, XRD and tensile tests. The results are summarized below:

- The density of the recycled filaments and the prints rises compared to the W/UR filament and print respectively.
- The crystallinity of the recycled filaments and the prints increases compared to the W/UR filament and print respectively.
- The tensile strength and modulus of the recycled filaments increases compared to the W/UR filament. The highest tensile strength and modulus are found for H1-3× recycled filament.

- The tensile strength and modulus of the recycled prints increase compared to the W/UR printed sample. The highest tensile strength and modulus are observed for the H1-3 × print.
- The H1-3 × print has exhibited superior tensile strength and modulus among all the recycled prints.

The present work successfully illustrated the recycling of nanocomposite waste filaments to minimize plastic waste. Through such an approach, as presented as part of this paper, the environmental pollution due to plastic waste generated by 3D printing industries can be substantially lowered in addition to expanding the filament material options for the FFF community. The H1 NCs have been printed without any warpage using suitable 3D printing parameters. Therefore, a similar route can be explored for other NCs (0.5, 1, 3 and 5 wt. % of the functionalized MWCNTs in the HDPE matrix), increasing the applications across various engineering fields such as structural, marine, aerospace and automobile.

Data availability Data is a part of the ongoing research work.

References

- Brauch HG, Spring ÚO, Mesjasz C, Grin J, Kameri-Mbote P, Chourou B, Dunay P, Birkmann J (2011) Coping with global environmental change, disasters and security: threats, challenges, vulnerabilities and risks, Vol. 5. Springer Science & Business Media
- Yoro KO, Daramola MO (2020) CO₂ emission sources, greenhouse gases, and the global warming effect, in *Advances in carbon capture*. Elsevier. p. 3–28
- Amaral SS, Costa MAM, Neto TGS, Costa MP, Dias FF, Anselmo E, Dos Santos JC, de Carvalho Jr JA (2019) CO₂, CO, hydrocarbon gases and PM_{2.5} emissions on dry season by deforestation fires in the Brazilian Amazonia. *Environm Pollut* 249:311–320
- Sekoai PT (2016) Yoro, Kelvin O Biofuel development initiatives in Sub-Saharan Africa: opportunities and challenges. *Climate* 4(2):33
- Yoro KO, Amosa MK, Sekoai PT, Mulopo J, Daramola MO (2020) Diffusion mechanism and effect of mass transfer limitation during the adsorption of CO₂ by polyaspartamide in a packed-bed unit. *Int J Sustain Eng* 13(1):54–67
- Yoro KO, Singo M, Mulopo JL, Daramola MO (2017) Modeling and experimental study of the CO₂ adsorption behaviour of polyaspartamide as an adsorbent during Post-combustion CO₂ capture. *Energy Procedia* 114:1643–1664
- Osler K, Oluwasina TN, OO, Daramola MO, (2017) Synthesis and performance evaluation of chitosan/carbon nanotube (chitosan/MWCNT) composite adsorbent for post-combustion carbon dioxide capture. *Energy Procedia* 114:2330–2335
- Hachimi T, Naboulsi N, Majid F, Rhanim R, Mrani I, Rhanim H (2021) Design and manufacturing of a 3D printer filaments extruder. *Procedia Str Integr* 33:907–916
- Atakok G, Kam M, Koc HB (2022) A review of mechanical and thermal properties of products printed with recycled filaments for use in 3d printers. *Surface Rev* 29(02):2230002
- Ukaogo PO, Ewuzie U, Onwuka CV (2020) Environmental pollution: causes, effects, and the remedies, in *Microorganisms for sustainable environment and health*. Elsevier. p. 419–429
- Khui PLN, Rahman MR, Jayamani E, Bakri MKB (2021) Recycling of sustainable polymers and composites, in *Advances in sustainable polymer composites*. Elsevier. p. 267–282
- Rahim TNAT, Abdullah AM, Md Akil H (2019) Recent developments in fused deposition modeling-based 3D printing of polymers and their composites. *Polymer Rev* 59(4):589–624
- Domingo-Espin M, Puigoriol-Forcada JM, Garcia-Granada A-A, Llumà J, Borros S, Reyes G (2015) Mechanical property characterization and simulation of fused deposition modeling Polycarbonate parts. *Mater Design* 83:670–677
- Lewenstam A, Bartoszewicz B, Migdalski J, Kochan A (2019) Solid contact reference electrode with a PVC-based composite electroactive element fabricated by 3D printing. *Electrochem Commun* 109:106613
- Mora A, Verma P, Kumar S (2020) Electrical conductivity of CNT/polymer composites: 3D printing, measurements and modeling. *Compos Part B Eng* 183:107600
- Rabbi MF, Chalivendra V (2020) Strain and damage sensing in additively manufactured CB/ABS polymer composites. *Polymer Test* 90:106688
- Exconde MJPC, Co JAA, Manapat JZ, Magdaluyo ER (2019) Materials selection of 3D printing filament and utilization of recycled polyethylene terephthalate (PET) in a redesigned breadboard. *Procedia CIRP* 84:28–32
- Gupta N, Zeltmann SE, Luong DD, Doddamani M (2019) Testing of foams, in *Handbook of mechanics of materials*. Springer Singapore. p. 2083–2122
- Ganesan S, Hemanandh J, Sridhar Raja, KS, Purusothaman M (2021) Experimental investigation and characterization of HDPE & LDPE polymer composites, in *Advances in Industrial Automation and Smart Manufacturing*. Springer. p. 785–799
- Singh AK, Patil B, Hoffmann N, Saltonstall B, Doddamani M, Gupta N (2018) Additive manufacturing of syntactic foams: part 1: development, properties, and recycling potential of filaments. *Addit Manufact Compos Complex Mater* 70(3):303–309
- Singh AK, Saltonstall B, Patil B, Hoffmann N, Doddamani M, Gupta N (2018) Additive manufacturing of syntactic foams: Part 2: Specimen printing and mechanical property characterization. *Addit Manufact Compos Complex Mater*. 70(3):310–314
- Patil B, Kumar BRB, Bontha S, Balla VK, Powar S, Kumar VH, Suresha SN, Doddamani M (2019) Eco-friendly lightweight filament synthesis and mechanical characterization of additively manufactured closed cell foams. *Compos Sci Technol* 183:107816
- Patil B, Kumar BRB, Doddamani M (2019) Compressive behavior of fly ash based 3D printed syntactic foam composite. *Mater Lett* 254:246–249
- Toutanji HA, Saafi M (2000) Flexural behavior of concrete beams reinforced with glass fiber-reinforced polymer (GFRP) bars. *Str J* 97(5):712–719
- Brenken B, Barocio E, Favalaro A, Kunc V, Pipes RB (2018) Fused filament fabrication of fiber-reinforced polymers: a review. *Addit Manufactur* 21:1–16
- Yuan Q, Bateman SA, Wu D (2010) Mechanical and conductive properties of carbon black-filled high-density polyethylene, low-density polyethylene, and linear low-density polyethylene. *J Thermoplast Compos Mater* 23(4):459–471
- Beesetty P, Patil B, Doddamani M (2020) Mechanical behavior of additively manufactured nanoclay/HDPE nanocomposites. *Compos Str* 247:112442
- Hu H, Zhang G, Xiao L, Wang H, Zhang Q, Zhao Z (2012) Preparation and electrical conductivity of graphene/ultrahigh molecular

- weight polyethylene composites with a segregated structure. *Carbon* 50(12):4596–4599
29. Amoroso L, Heeley EL, Ramadas SN, McNally T (2020) Crystallisation behaviour of composites of HDPE and MWCNTs: The effect of nanotube dispersion, orientation and polymer deformation. *Polymer* 201:122587
 30. Bharath HS, Bonthu D, Gururaja S, Prabhakar P, Doddamani M (2021) Flexural response of 3D printed sandwich composite. *Compos Str* 263:113732
 31. Bonthu D, Bharath HS, Gururaja S, Prabhakar P, Doddamani M (2020) 3D printing of syntactic foam cored sandwich composite. *Compos Part C* 3:100068
 32. Vashishtha VK, Makade R, Mehla N (2011) Advancement of rapid prototyping in aerospace industry—a review. *Int J Eng Sci Technol* 3(3):2486–2493
 33. Bharath Kumar BR, Doddamani M, Zeltmann SE, Gupta N, Gurupadu S, Sailaja RRN (2016) Effect of particle surface treatment and blending method on flexural properties of injection-molded cenosphere/HDPE syntactic foams. *J Mater Sci* 51(8):3793–3805
 34. Valvez S, Santos P, Parente JM, Silva MP, Reis PN (2020) 3D printed continuous carbon fiber reinforced PLA composites: A short review. *Procedia Str Integrity* 25:394–399
 35. Dileep B, Doddamani M (2021) Compressive response of 3D printed graded foams. *Compos Part C Open Access*. 6:100181
 36. Bharath HS, Bonthu D, Prabhakar P, Doddamani M (2020) Three-dimensional printed lightweight composite foams. *ACS Omega* 5(35):22536
 37. Dileep B, Prakash R, Bharath HS, Jeyaraj P, Doddamani M (2021) Dynamic behavior of concurrently printed functionally graded closed cell foams. *Compos Str* 275:114449
 38. Liu Y, Asare E, Porwal H, Barbieri E, Goutianos S, Evans J, Newton M, Busfield JJ, Peijs T, Zhang H, Bilotti E (2020) The effect of conductive network on positive temperature coefficient behaviour in conductive polymer composites. *Compos A Appl Sci Manuf* 139:106074
 39. Stan F, Stanciu NV, Fetecau C (2019) On the 3D printability of multi-walled carbon nanotube/high density polyethylene composites. *Int Manuf Sci Eng Conference Am Soc Mechan Eng*. <https://doi.org/10.1115/MSEC2019-2776>
 40. Behera RP, Rawat P, Tiwari SK, Singh KK (2020) A brief review on the mechanical properties of Carbon nanotube reinforced polymer composites. *Mater Today Proc* 22:2109–2117
 41. Tang W, Advani SMH, SG, (2003) Melt processing and mechanical property characterization of multi-walled carbon nanotube/high density polyethylene (MWNT/HDPE) composite films. *Carbon* 41(14):2779–2785
 42. Kumar S, Ramesh MR, Doddamani M, Rangappa SM, Siengchin S (2022) Mechanical characterization of 3D printed MWCNTs/HDPE nanocomposites. *Polym Testing* 114:107703
 43. Fouad H, Elleithy R, Al-Zahrani SM, Ali MA (2011) Characterization and processing of high density polyethylene/carbon nanocomposites. *Mater Design* 32(4):1974–1980
 44. Adhikary KB, Park CB, Islam MR, Rizvi GM (2011) Effects of lubricant content on extrusion processing and mechanical properties of wood flour-high-density polyethylene composites. *J Thermoplast Compos Mater* 24(2):155–171
 45. Di W, Zhang G, Xu J, Peng Y, Wang X, Xie Z (2003) Positive-temperature-coefficient/negative-temperature-coefficient effect of low-density polyethylene filled with a mixture of carbon black and carbon fiber. *J Polym Sci* 41(23):3094–3101
 46. Dabees S (2021) Tirth, Vineet, Mohamed, Alaa, Kamel, Bahaa M, *Wear performance and mechanical properties of MWCNT/HDPE nanocomposites for gearing applications*. *J Market Res* 12:2476–2488
 47. Singh R, Singh H, Farina I, Colangelo F, Fraternali F (2019) On the additive manufacturing of an energy storage device from recycled material. *Compos Part B Eng* 156:259–265
 48. Singh N, Singh R, Ahuja IPS (2018) Recycling of polymer waste with SiC/Al₂O₃ reinforcement for rapid tooling applications. *Mater Today Commun* 15:124–127
 49. Stan F, Stanciu NV, Fetecau C, Sandu IL (2019) Mechanical recycling of low-density polyethylene/carbon nanotube composites and its effect on material properties. *J Manuf Sci Eng* 141(9):091004
 50. Fang C, Yang R, Zhang Z, Zhou X, Lei W, Cheng Y, Zhang W, Wang D (2018) Effect of multi-walled carbon nanotubes on the physical properties and crystallisation of recycled PET/TPU composites. *J RSC Adv* 8(16):8920–8928
 51. Singh R, Singh N, Fabbrocino F, Fraternali F, Ahuja IP (2016) Waste management by recycling of polymers with reinforcement of metal powder. *Compos Part B Eng* 105:23–29
 52. Kumar S, Ramesh MR, Doddamani M (2022) Compressive behavior of 3D printed MWCNT/HDPE nanocomposites. *Compos Commun* 35:101317
 53. Doddamani M (2020) Dynamic mechanical analysis of 3D printed eco-friendly lightweight composite. *Compos Commun* 19:177–181
 54. Jayavardhan ML, Kumar BB, Doddamani M, Singh AK, Zeltmann SE, Gupta N (2017) Development of glass microballoon/HDPE syntactic foams by compression molding. *Compos Part B Eng* 130:119–131

Publisher's Note Springer Nature remains neutral with regard to jurisdictional claims in published maps and institutional affiliations.

Springer Nature or its licensor (e.g. a society or other partner) holds exclusive rights to this article under a publishing agreement with the author(s) or other rightsholder(s); author self-archiving of the accepted manuscript version of this article is solely governed by the terms of such publishing agreement and applicable law.